News from the WOCE IPO

W. John Gould, Director, WOCE IPO and ICPO, Southampton Oceanography Centre, UK. john.gould@soc.soton.ac.uk

Not Long to go Now

Lots of things that I have been dealing with over the period since the last Newsletter have been about activities needed to bring WOCE to a conclusion by the end of 2002. Let me tell you about them.

That Book!

Firstly I have been sending off to Academic Press the completed Chapters for the "WOCE" book now titled "Ocean Circulation and Climate – Observing and Modelling the Global Ocean". Of the 33 Chapters only about 3 need a little more work before they are submitted. All will be completed by the time this newsletter appears on your desks. Unfortunately I still cannot give you information about the price of the book. That will be fixed in September when the publishers have put it all together. It has been an enormous undertaking for the authors, for staff in Hobart and for Roberta Boscolo and Jean Haynes in the WOCE IPO. Gerold Siedler and John Church and I as editors are pleased to see it finally coming together.

Workshops

Today I sent out a final reminder about the deadline for submitting abstracts for the WOCE Workshop in Fukuoka on Variability and Representativeness of the WOCE data sets. We are looking forward to a stimulating meeting. The workshop is co-sponsored by CLIVAR and will provide some important pointers for the ocean sampling strategy that CLIVAR will need to adopt.

There is only one more workshop scheduled in the WOCE AIMS series and that is the one at which the estimates of oceanic transports of heat, freshwater and chemical constituents will be discussed. It will also make progress towards deciding what those transports were during

Impact of 4D-Variational Assimilation of WOCE Hydrography on the Meridional Overturning Circulation of the Indian Ocean

Bruno Ferron, Laboratoire de Physique des Océans, France; and
Jochem Marotzke, Southampton Oceanography Centre, UK.
Bruno.Ferron@ifremer.fr

The deep meridional overturning circulation of the Indian Ocean still represents a dilemma to oceanographers. Estimates either from hydrographic sections or from general circulation models (GCMs) differ significantly in the structure and rate of the overturning. Depending on hydrographic lines considered and details of inverse methods used, the northward transport below 2000 m ranges from $3.6 \times 10^6 \, \text{m}^3\text{s}^{-1}$ (Fu, 1986) up to $(27 \pm 10) \times 10^6 \, \text{m}^3\text{s}^{-1}$ (Toole and Warren, 1993). The most recent estimate from Ganachaud et al. (2000), which includes recent WOCE sections, gives a deep inflow of $(11 \pm 4) \times 10^6 \, \text{m}^3\text{s}^{-1}$. In contrast, GCMs only produce weak deep overturnings (Wacongne and Pacanowski, 1996; Lee and Marotzke, 1997, 1998; Garternicht and Schott, 1997; Zhang and Marotzke, 1999).

Inconsistencies between the two type of estimates may be attributed to deficiencies of either of the methods. On the one hand, inverse model results depend on error estimates which should in principle include errors present in the model itself. For instance, inverse models typically assume steady state, whereas the Indian Ocean has a strong seasonal cycle and has probably an interannual cycle due to El Niño events. This temporal variability has to be part of errors in the inversion process, especially when the inversion combines several hydrographic lines taken at different seasons or years (Ganachaud et al., 2000, include this variability in their error estimates). On the other hand, GCMs are initialised from climatologies which are smoothed and miss the real thermal wind. Integrating in time perfect GCMs with perfect forcings would probably converge to what is observed even if the spin-up is done from a climatology. But forcing fields are far from perfect, and the subgrid-scale physics of GCMs are parameterised. Hence, GCMs may fail to represent the basic circulation of the Indian Ocean circulation.

In order to test whether initial conditions closer to observations change the deep circulation of a GCM, we present here some preliminary results of a 4D-variational approach which combines the dynamics of a GCM and the WOCE hydrography. The assimilation changes some independent variables (e.g. initial conditions) of the GCM to correct the trajectory of the model so that the resulting estimated circulation (i.e. dynamics) is consistent with observations within some error bars.
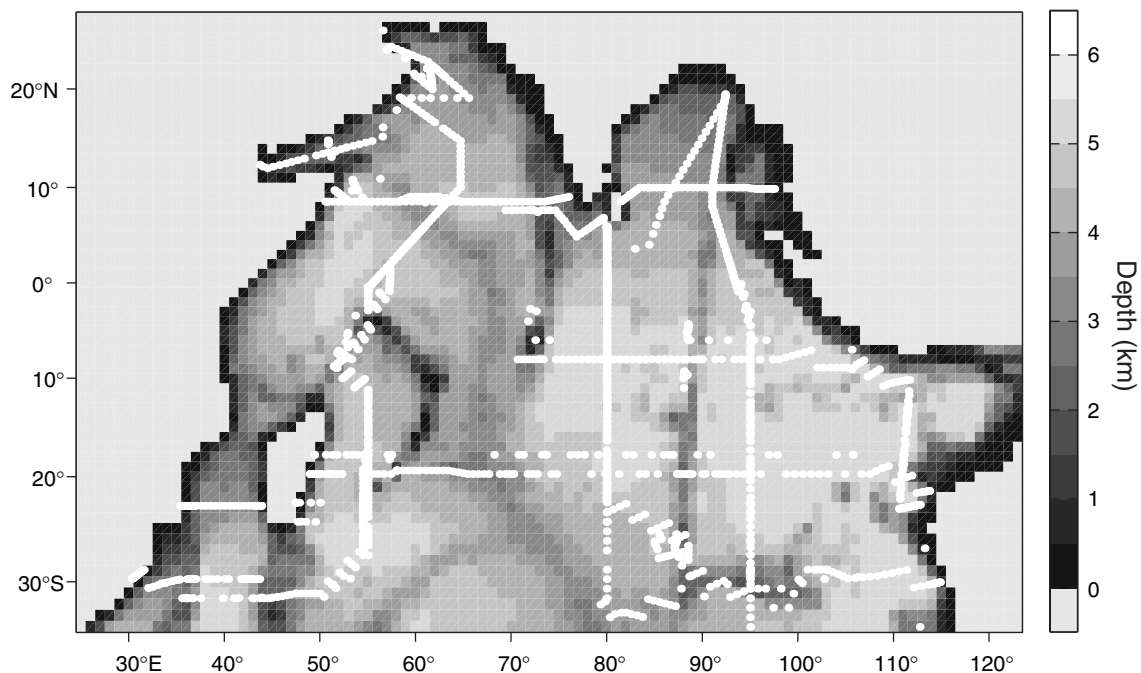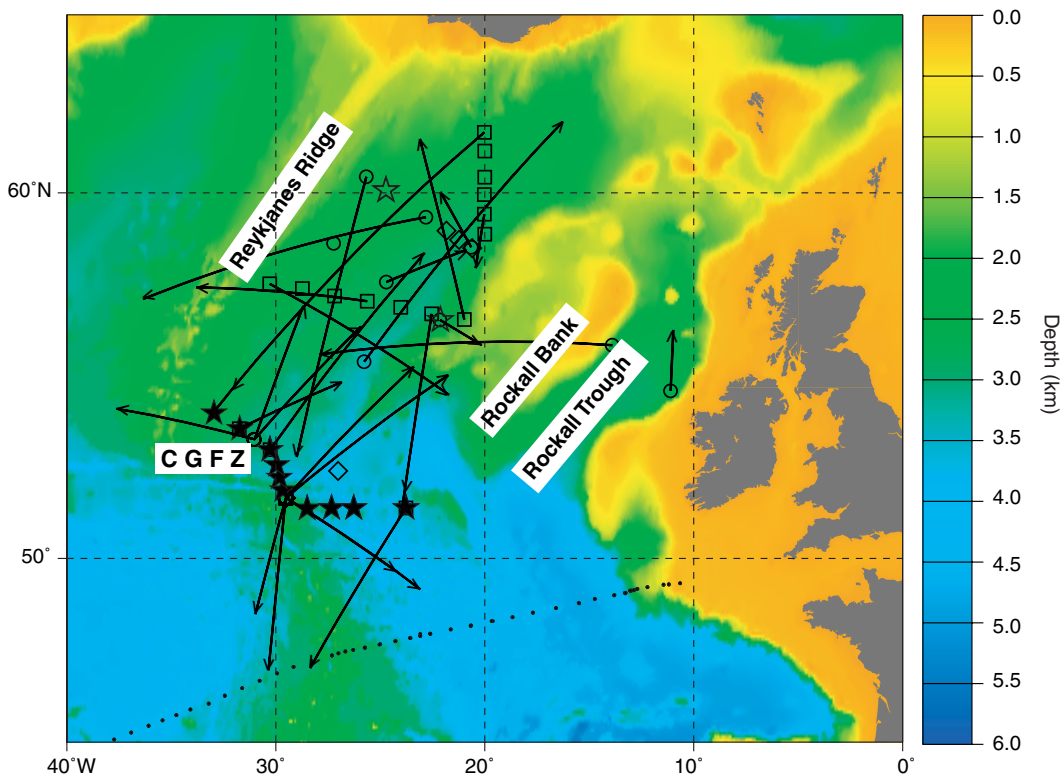

Figure 1. Gridded bathymetry of the model and the WOCE CTDs collected during 1995 (white dots).

Zenk, page 3, *Figure 1. Topographic chart of the Iceland Basin. Included are locations featuring RAFOS sound sources (open stars) and current meter mooring sites (bold stars), launch (open symbols) and surface positions (arrow tips) from three float seeding cruises according to Tables 1 and 2. On the average displacement vectors represent mission length of 15 months. The lower dotted line denotes WOCE section A2.*
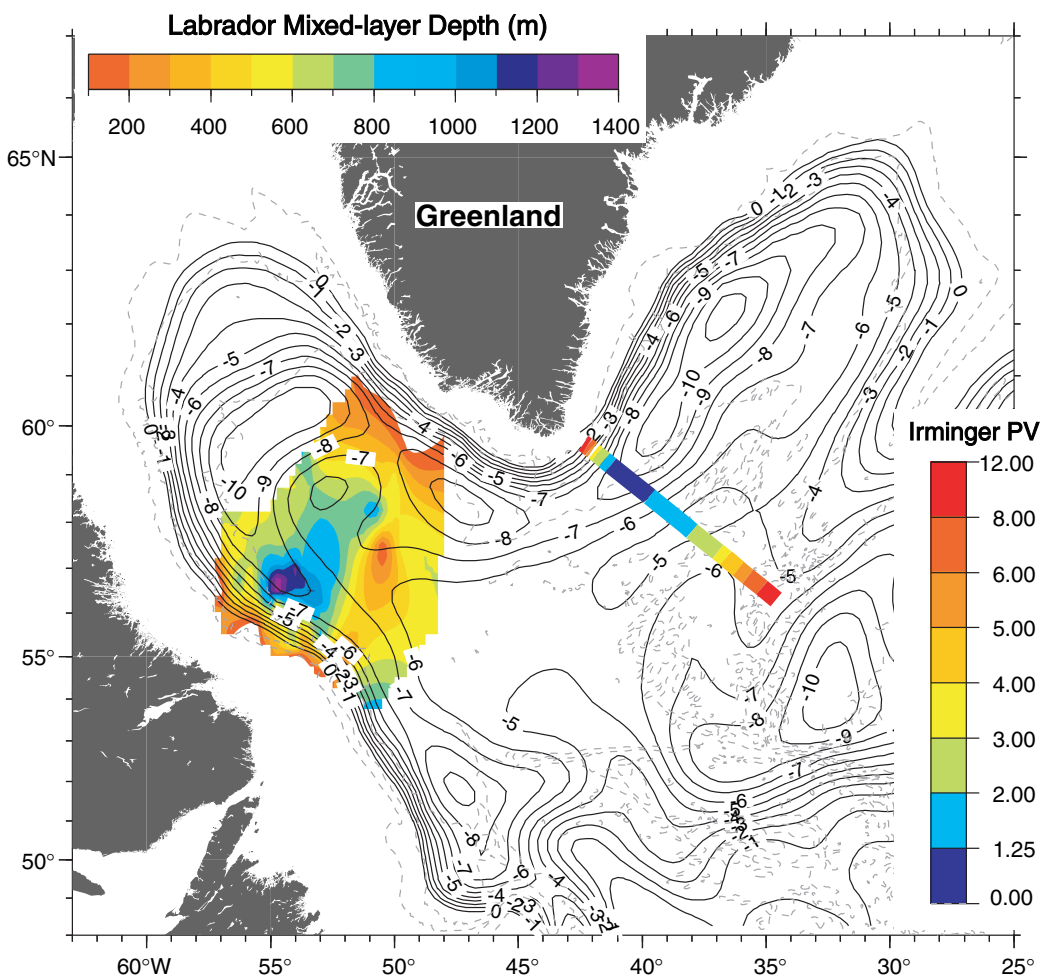

Pickart and Lavender, page 6, *Figure 1. Absolute geostrophic pressure at 700 m (contours in cm) from Lavender et al. (2000). Overlaid on this is the Labrador Sea mixed-layer depth (m) in winter 1997, and the average potential vorticity $(1/(ms) \times 10^{-12})$ of the LSW in the Irminger Sea during the 1990s (see text).*
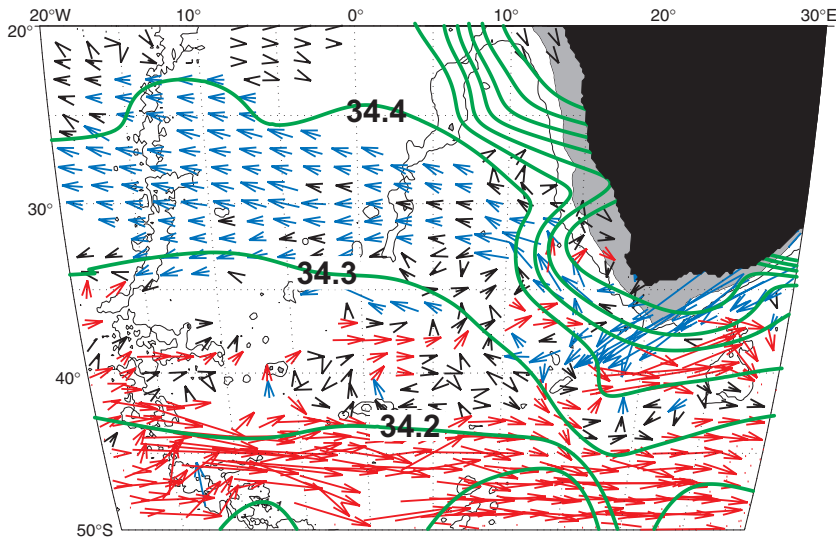
Boebel et al., page 9, *Figure 3. Mean flow and superposed salinity on* $\sigma_\theta = 27.2$ *surface. Arrows are black if speeds are less than* $2.5\,cm\,s^{-1}$ *and in colour if greater. Red and blue arrows indicate eastward and westward zonal components, respectively. Green lines indicate isohalines.*
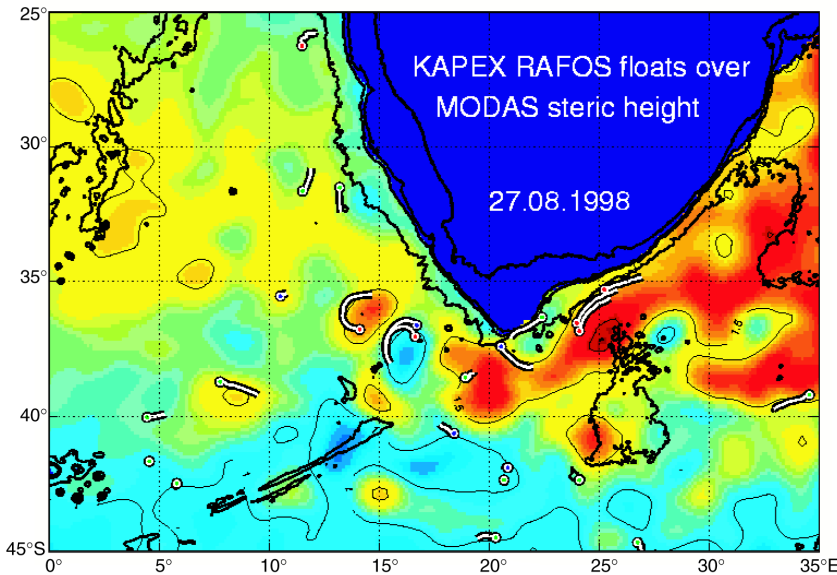

Boebel et al., page 9, *Figure 4. KAPEX RAFOS float trajectories over MODAS steric height anomaly. Trajectory segments span 7 days centred on 27 August 1998. A trajectory segment of 1° length corresponds to a velocity of* $18\,cm\,s^{-1}$. *Thick solid lines represents isobaths at 0, 500, 1000 and 3000 m depth. Steric height anomaly contours (thin black lines) are at 1, 1.5 and 2 m, located over cyan, yellow and red background colour respectively. This movie can be downloaded by anonymous ftp (39 Mbytes) from pogo.gso.uri.edu/ pub/oboebel/agulhas_movie.zip.*
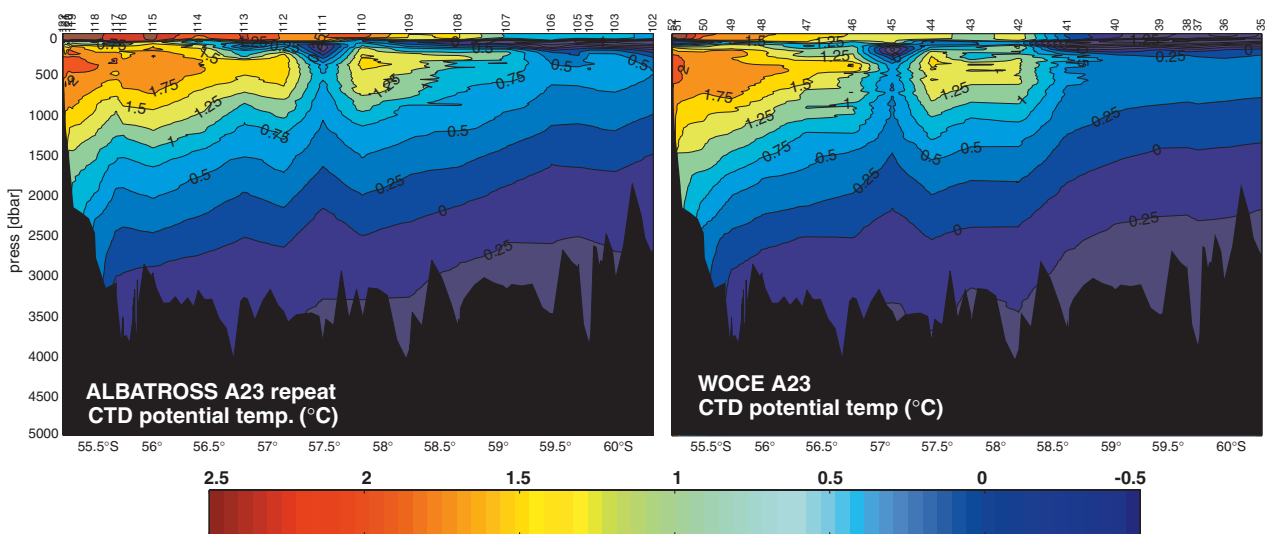
**Meredith et al., page 15,** *Figure 2. Potential temperature in the eastern Scotia Sea from CTD measurements. Right panel is from the WOCE section A23 in 1995; left panel is from the ALBATROSS cruise in 1999. Station locations are marked by cruise station numbers above the uppermost horizontal axis.*

Fox et al., page 27, *Figure 3. OCCAM temperature deviations after one year for (a) the ECMWF 6-hourly wind run, and (b) the smoothed wind run. Deviations are relative to the reference run driven by monthly climatological winds and show the effects of internal waves on deep ocean mixing in OCCAM.*
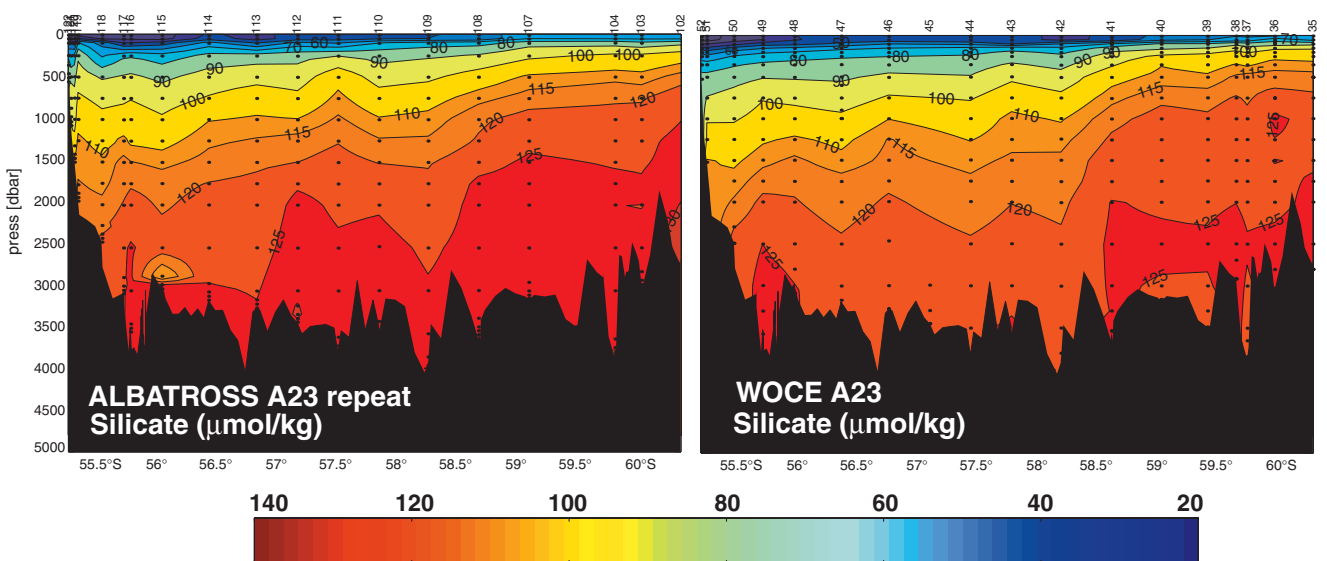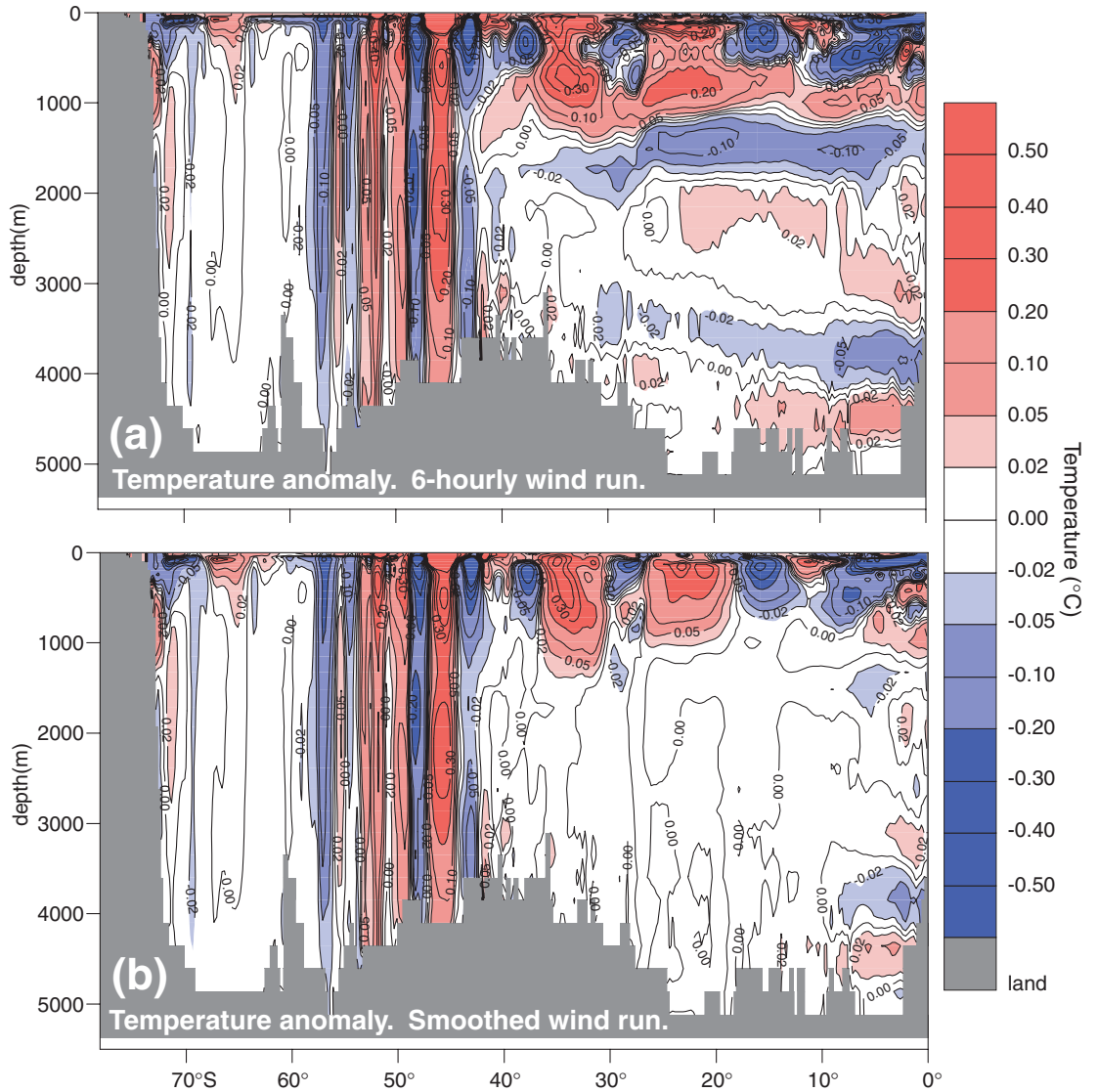
Meredith et al., page 15, *Figure 5. As for Fig. 2, but for dissolved silicate. Locations of discrete water samplings are marked with dots.*
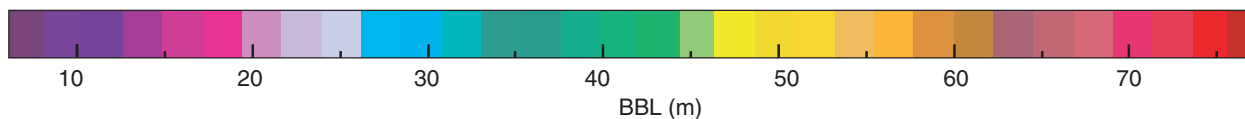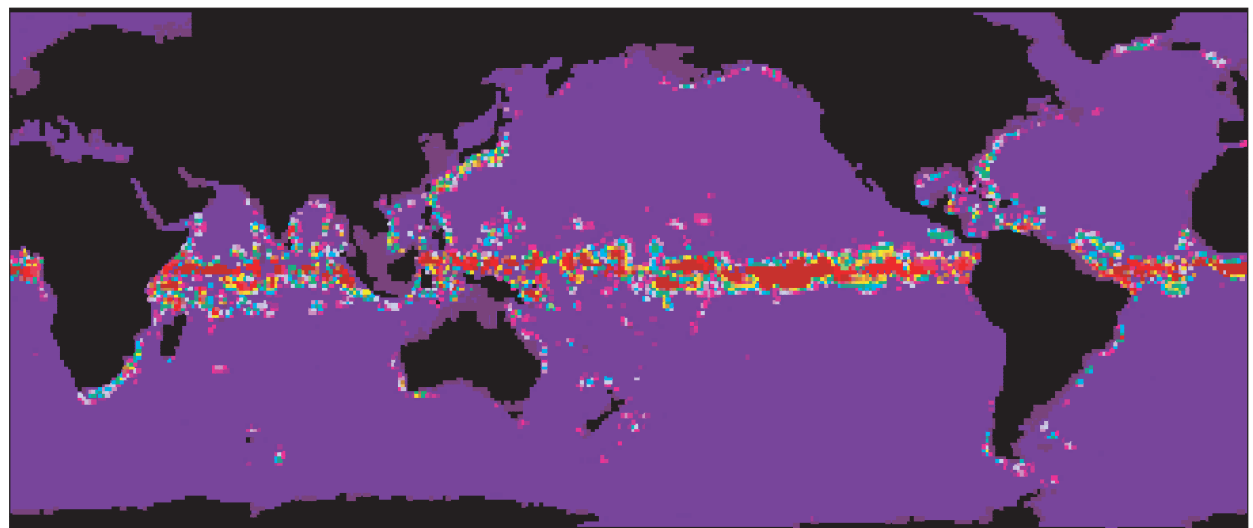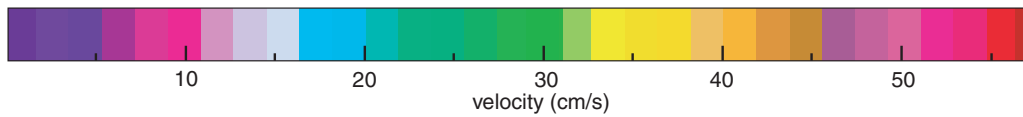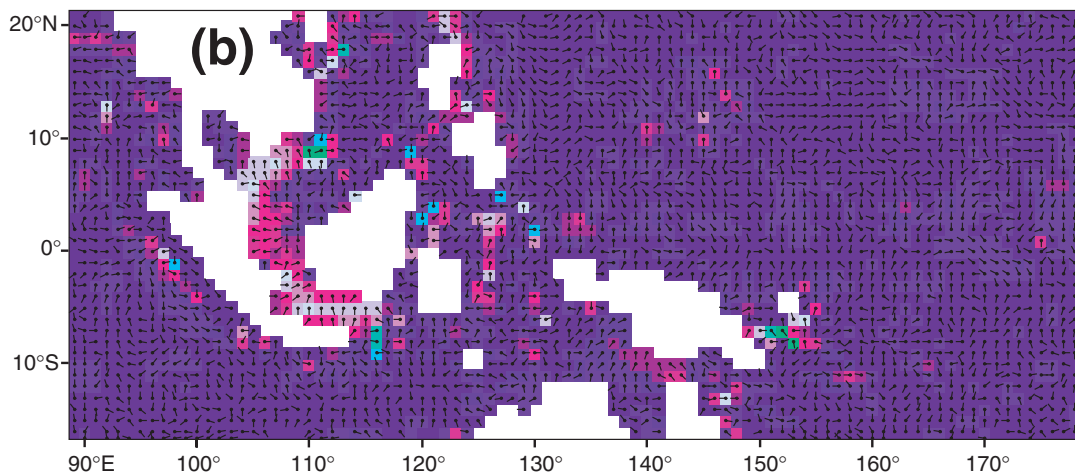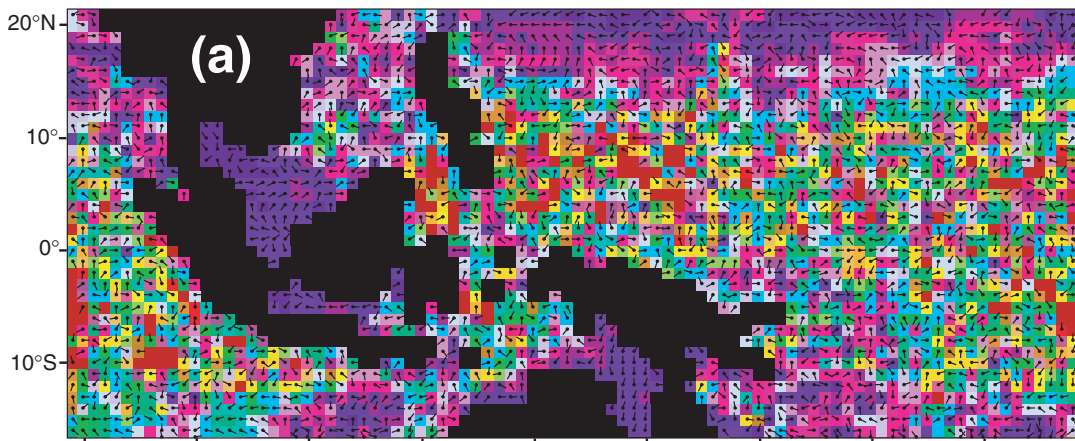
Nurser et al., page 34, *Figure 3. BBL velocity field for (a) standard Killworth and Edwards run (direction of arrow from blob shows direction of flow; colour scale shows speed in cm s⁻¹) (b) BBL velocity field using new pressure gradient formulation.*

Nurser et al., page 34, *Figure 4. Global plot of BBL thickness, in m.*

Configuration of the model - Spin-up

We use Marshall et al. (1997a,b) primitive equation model (also known as MIT model). Its adjoint is derived with the Tangent Linear and Adjoint Model Compiler (Giering and Kaminski, 1998), as described in Marotzke et al. (1999). The resolution is $1° \times 1°$ horizontally with 23 vertical levels. The model uses Laplacian diffusion in the horizontal and the vertical. A convective algorithm ensures a stable stratification. The domain is regional (Fig. 1); open boundaries are prescribed at 35°S (South Africa–Australia) and 122°E (Indonesian Throughflow) and conserve the Indian Ocean volume. Velocity fields at the open boundary are interpolated from Stammer et al.'s (1997) global assimilation. The surface forcing comes from the National Center for Environmental Prediction (NCEP). Since most of the WOCE hydrography (CTDs) of the Indian Ocean was measured during year 1995, surface and lateral forcing correspond also to year 1995.

The model is spun up from rest, with T and S in the interior and at the open boundaries taken from Levitus. The model undergoes 10 cycles of slightly modified year-1995 forcing. The first-guess initial conditions used in the subsequent optimisation corresponds to the end of year 4 of the spin-up.

Control variables - Cost function

The control vector XX represents the independent variables that are modified to obtain a better fit of the GCM with observations. XX is composed of open boundaries, surface forcings and the first guess (i.e. the initial conditions on T, S, U and V).

The cost function measures the misfit between the model and WOCE CTD data, weighted by some specified variances, but also measures the magnitude of the XX. Errors in the hydrography were calculated as variances of CTD temperature and salinity within a model grid box to account for the coarse resolution of our model. A background error is added to represent the effect of internal waves on CTD data. Errors in the wind stress

are computed from statistics between NCEP and ERS products. Errors in the heat and in the evaporation–precipitation are constant over the domain. Since the modelled temperature and salinity deviate significantly from

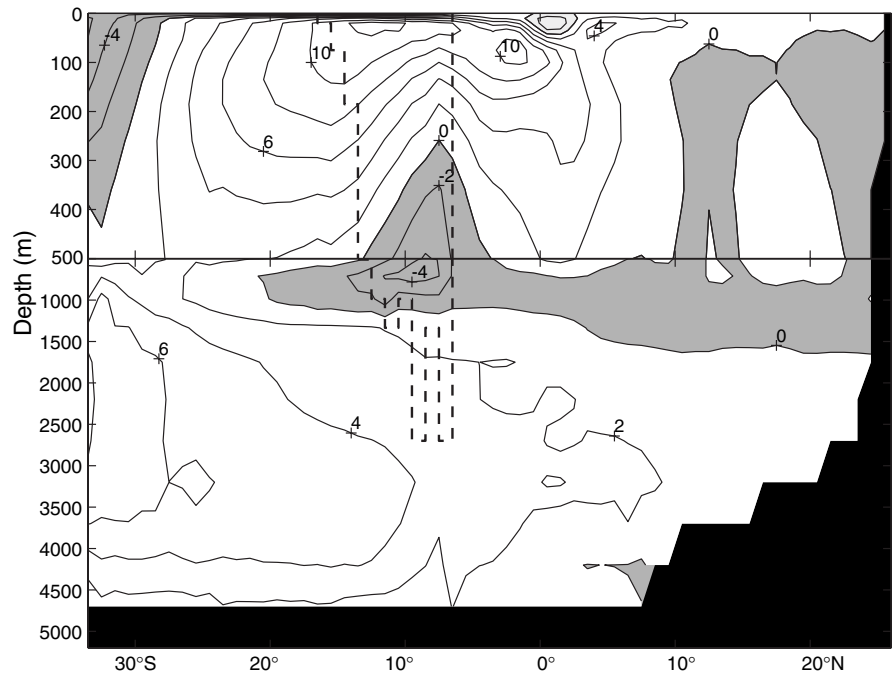*Figure 2. Annual mean meridional overturning after a 5-year spin-up started from Levitus fields and Stammer (1997)'s velocity fields at the open boundaries (positive = counter-clockwise). The dashed lines indicate the location of the Indonesian Throughflow.*
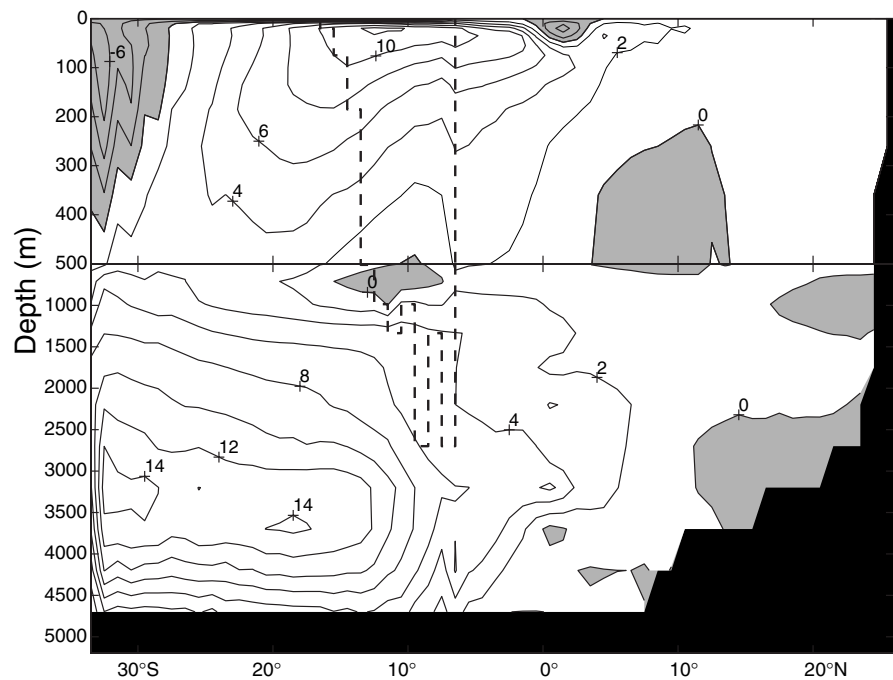

Figure 3. Estimated annual mean meridional overturning after the assimilation of WOCE CTD data (12 iterations with the forward and adjoint models).

observations, the assumed error in the first guess is large; hence it is downweighted. Temperature and salinity at the open boundaries are also weakly constrained which is not the case for velocities at the open boundaries.

Preliminary results

Fig. 2 presents the a priori annual mean meridional overturning based on an average of the monthly fields. Note that in the region of the Indonesian Throughflow which carries $4.5 \times 10^6 \text{ m}^3 \text{s}^{-1}$ westward (area bounded by the dashed line), the flow is divergent and isolines represent constant transports integrated from the bottom. Our first guess is similar to previous studies. The circulation is intensified in the first 1000 m with a weak overturning cell at depth. The southern open boundary tries to force a deep overturning of $8 \times 10^6 \text{ m}^3 \text{s}^{-1}$

Figure 4. Difference between the estimated and the a priori overturning circulations.

but the interior flow does not allow for more than $4 \times 10^6 \text{ m}^3 \text{s}^{-1}$ north of 27°S.

Fig. 3 shows the meridional circulation obtained after a three year-run started from the new initial conditions and forcings generated by twelve iterations of assimilation. The estimated solution is not statistically consistent yet (especially in the first hundred metres), although it is three times more consistent than the first guess. The deep circulation is remarkably modified after the assimilation of WOCE hydrography as Fig. 3 shows. The deep overturning now reaches more than $12 \times 10^6 \text{ m}^3 \text{s}^{-1}$ and penetrates up to 12°S. Other experiments based on different constraints (i.e. error bars) on the first guess fields and different initial conditions systematically develop a deep overturning of more than $10 \times 10^6 \text{ m}^3 \text{s}^{-1}$. Such a pattern for the deep circulation of the Indian Ocean is consistent with the hydrographic inversions calculated by Robbins and Toole (1997), Macdonald (1995) and Ganachaud et al. (2000). The significant contrast in the deep circulation between the previous GCM circulations and ours emphasises the drawbacks of smoothed climatologies and the difficulties of GCMs to improve it even when integrated over long timescales.

The difference between the estimated and the a priori overturning circulations (Fig. 4) shows that the CTD data have mainly modified the deep circulation. However, one can note a significant weakening of the circulation at and north of the Equator. The few modifications brought to the upper ocean may be attributed to the shorter correlation time of the circulation at the surface compared to what is observed at depth. Because of limitations in adjoint derivations, our model is too simplistic in the surface physics parameterisation. Hence, this could also limit the impact of assimilating CTDs in the upper ocean, since the
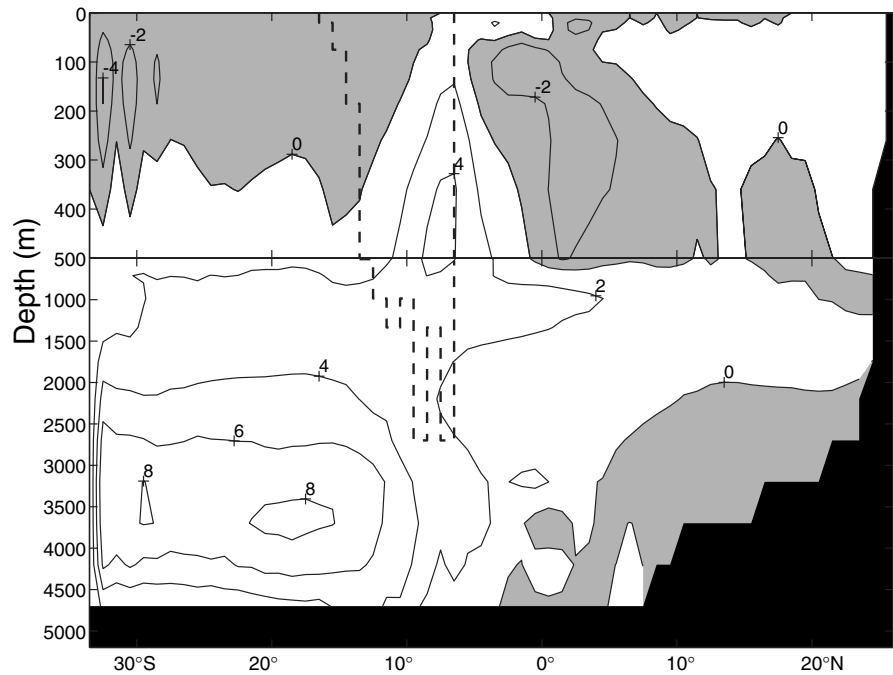
assimilation may try to correct for the coarse physics. A better upper ocean physics would exploit the CTD data to a higher degree. Moreover, the lack of upper ocean physics is not taken into account in the variances that weight the model-data misfit. This may explain the statistical inconsistency we observe in the first ocean levels. Choosing variances adequately with the upper ocean physics of the GCM may solve the statistical consistency issue. This work is still ongoing. Although CTDs did not produce any significant change in the Indonesian Throughflow (Fig. 3 shows that open boundaries are weakly constrained by the CTD data), first results from the inclusion of altimetric data in the assimilation seems to be promising for constraining the open boundaries. Details of this study will be published elsewhere.

Acknowledgements

References

Fu, L.-L., 1986: Mass, heat and freshwater fluxes in the south Indian Ocean. J. Phys. Ocean., 16, 1683–1693.

Ganachaud, A., C. Wunsch, J. Marotzke, and J. Toole, 2000: The meridional overturning and large-scale circulation of the Indian Ocean. J. Geophys. Res., in press.

Garternicht, U., and F. Schott, 1997: Heat fluxes of the Indian Ocean from a global eddy-resolving model. J. Geophys. Res., 102, 21147–21159.

Giering, R., and T. Kaminski, 1998: Recipes for adjoint code construction. ACM Trans. Math., 24, 437–474.

Lee, T., and J. Marotzke, 1997: Inferring meridional mass and heat transports in the Indian Ocean by combining a general circulation model with climatological data. J. Geophys. Res., 102, 10585–10602.

Lee, T., and J. Marotzke, 1998: Seasonal cycles of meridional overturning and heat transport of the Indian Ocean. J. Phys. Ocean., 28, 923–943.

Macdonald, A., 1995: Oceanic fluxes of mass, heat, and freshwater: a global estimate and perspective. PhD dissertation. MIT/WHOI Joint Program in Oceanography. 326 pp.

Marotzke, J., R. Giering, K. Q. Zhang, D. Stammer, C. Hill, and T. Lee, 1999: Construction of the adjoint MIT ocean general circulation model and application to Atlantic heat transport sensitivity. J. Geophys. Res., 104, 29529–29547.

Marshall, J., C. Hill, L. Perelman, and A. Adcroft, 1997a: Hydrostatic, quasi-hydrostatic, and non-hydrostatic ocean modeling. J. Geophys. Res., 102, 5733–5752.

Marshall, J., A. Adcroft, C. Hill, L. Perelman, and C. Heisey, 1997b: A finite-volume, incompressible Navier-Stokes model for studies of the ocean on parallel computers. J. Geophys. Res., 102, 5753–5766.

Robbins, P. E., and J. M. Toole, 1997: The dissolved silica budget as a constraint on the meridional overturning circulation of the Indian Ocean. Deep-Sea Res., 44, 879–906.

Stammer, D., C. Wunsch, R. Giering, Q. Zhang, J. Marotzke, J. Marshall, and C. Hill, 1997: The global ocean circulation estimated from TOPEX/POSEIDON altimetry and a general circulation model. Center for Global Change Science Report, 49, MIT, 40 pp.

Toole, J. M., and B. A. Warren, 1993: A hydrographic section across the subtropical south Indian Ocean. Deep-Sea Res., 40, 1973–2019.

Wacongne, S., and R. Pacanowski, 1996: Seasonal heat transport in a primitive equations model of the tropical Indian Ocean. J. Phys. Oceanogr., 26, 2666–2699.

Zhang, Q., and J. Marotzke, 1999: The importance of open-boundary estimation for an Indian Ocean gcm-data synthesis. J. Mar. Res., 57, 305–334.

Modelling Internal Waves with a Global Ocean Model

Alan D. Fox and Keith Haines, Department of Meteorology, University of Edinburgh, UK; and Beverly A. de Cuevas, Southampton Oceanography Centre, UK.
A.D.Fox@ed.ac.uk

Internal inertia-gravity waves are a ubiquitous feature of the oceans existing on spatial scales from tens of metres up to hundreds of kilometres, and with timescales ranging from a few minutes to the local inertial period. Such waves are generated by the action of the wind at the surface and by the interaction of currents – both tidal and wind-driven – with topography. Whatever the mechanism producing the internal waves, arguably their most important role in ocean circulation is in energy transport. For example, energy input by the wind at the surface can be transported to the deep ocean where it is dissipated in turbulence and mixing. This deep ocean mixing in turn forms an important component of the ocean general circulation. In this way internal waves, although small-scale, influence the largest scales of motion in the ocean.

Until recently the resolution of global ocean general circulation models has been too coarse to resolve even the largest scales of internal waves. Together with global models being almost exclusively run with no tidal currents and purely low-frequency wind forcing, this produces models with little or no internal wave activity. The representation of the effects of internal waves is therefore limited to parameterisations of sub-gridscale processes. However, with increasing computer power, global models are now being run which are able to resolve the large-scale, low-frequency part of the internal wave spectrum. When driven with high-frequency global wind fields these models then contain an explicit representation of the near-inertial frequency, wind-driven part of the internal wave spectrum. Here we describe some results obtained by forcing the UK NERC OCCAM (Ocean Circulation and Climate Advanced Modelling project) $\frac{1}{4}°$ global ocean model with ECMWF 6-hourly global wind fields. First it is useful to highlight some important features of the near-inertial frequency internal wave field in the ocean.

Observations of inertial waves in the ocean

Current meter records demonstrate the presence of internal waves at all depths in the ocean. These observations show a peak in the energy spectrum at frequencies just above the inertial frequency, f. These are generally termed near-inertial frequency waves, or 'inertial waves'. Observation and theory reveal the following basic characteristics of inertial waves (for more details see for example Fu, 1981; Gill, 1982):

1. Generation is predominantly by travelling wind fields, for example eastward moving depressions. This surface generation is confirmed by the dominant downward energy propagation.

2. Currents are almost horizontal (purely horizontal when $\omega = f$) and rotate with time in an anticyclonic direction. Current speeds can be as high $70\,\mathrm{cm\,s^{-1}}$ in the surface layer, decreasing with depth below the thermocline to $3-4\,\mathrm{cm\,s^{-1}}$ near the bed (Sanford, 1975). Vertical displacements of tens of metres in the thermocline have been commonly observed.

3. Intermittent – waves are observed to persist locally for 3–20 wave periods, this observation does not preclude waves persisting for longer periods having